0022-3565/09/3301-40–53$20.00
THE JOURNAL OF PHARMACOLOGY AND EXPERIMENTAL THERAPEUTICS
JPET 330:40–53, 2009

Vol. 330, No. 1
151225/3479994
Printed in U.S.A.

Differential Regulation of Receptor Activation and Agonist Selectivity by Highly Conserved Tryptophans in the Nicotinic Acetylcholine Receptor Binding Site

Dustin K. Williams, Clare Stokes, Nicole A. Horenstein, and Roger L. Papke

Department of Pharmacology and Therapeutics, University of Florida College of Medicine, Gainesville, Florida (D.K.W., C.S., R.L.P.); and Department of Chemistry, University of Florida, Gainesville, Florida (N.A.H.)

Received January 22, 2009; accepted March 30, 2009

ABSTRACT

We have shown previously that a highly conserved Tyr in the nicotinic acetylcholine receptor (nAChR) ligand-binding domain (LBD) (α7 Tyr188 or α4 Tyr195) differentially regulates the activity of acetylcholine (ACh) and the α7-selective agonist 3-(4-hydroxy,2-methoxybenzylidene)anabaseine (4OH-GTS-21) in $\alpha4\beta2$ and α7 nAChR. In this study, we mutated two highly conserved LBD Trp residues in human α7 and $\alpha4\beta2$ and expressed the receptors in *Xenopus laevis* oocytes. α7 Receptors with Trp55 mutated to Gly or Tyr became less responsive to 4OH-GTS-21, whereas mutation of the homologous Trp57 in β2 to Gly, Tyr, Phe, or Ala resulted in $\alpha4\beta2$ receptors that showed increased responses to 4OH-GTS-21. Mutation of α7 Trp55 to Val resulted in receptors for which the partial agonist 4OH-GTS-21 became equally efficacious as ACh, whereas $\alpha4\beta2$ receptors with the homologous mutation remained non-responsive to 4OH-GTS-21. In contrast to the striking alterations in agonist activity profiles that were observed with mutations of α7 Trp55 and β2 Trp57, mutations of α7 Trp149 or α4 Trp154 universally resulted in receptors with reduced function. Our data support the hypothesis that some conserved residues in the nAChR LBD differentially regulate receptor activation by subtype-selective agonists, whereas other equally well conserved residues play fundamental roles in receptor activation by any agonist. Residues like α7 Trp149 (α4 Trp154) may be considered pillars upon which basic receptor function depends, whereas α7 Trp55 (β2 Trp57) and α7 Tyr188 (α4 Tyr195) may be fulcra upon which agonists may operate differentially in specific receptor subtypes, consistent with the hypothesis that ACh and 4OH-GTS-21 are able to activate nAChR in distinct ways.

The Cys-loop superfamily of ligand-gated ion channels, which includes channels gated by acetylcholine (ACh), serotonin, γ-aminobutyric acid, and Gly, has been hypothesized to have evolved from a common ancestor (Ortells and Lunt, 1995). Sequence analysis of receptor subunits within the Cys-loop superfamily, all the way through to prokaryotic ligand-gated ion channels, illustrates remarkable conservation at select sites and have implicated great functional significance to aromatic residues localized in the ligand-binding domain (LBD) of receptors within the Cys-loop superfamily (Tasneem et al., 2005). In nicotinic acetylcholine receptors (nAChRs), Trp55 and Trp149 (α7 numbering) have been identified among other aromatic ring-containing residues as highly conserved throughout evolution and as contributors to the formation of a hydrophobic LBD (Cohen et al., 1991; Tomaselli et al., 1991; Devillers-Thiéry et al., 1993; Aylwin and White, 1994; Galzi and Changeux, 1995; Chiara and Cohen, 1997; Chiara et al., 1998; Brejc et al., 2001; Xiu et al., 2009).

Several studies have shown that mutation of highly conserved aromatic residues typically results in decreased efficacy and/or potency for ACh and related ammonium compounds (Galzi et al., 1991; O'Leary and White, 1992; Sine et al., 1994; Xie and Cohen, 2001). However, observations by Horenstein et al. (2007) suggest that mutation of conserved aromatic residues may not result in loss of receptor activity for all ligands, and conserved aromatic residues may differentially regulate receptor activation by select agonists. Specifically, the activation of human α7 nAChR by 3-(4-hydroxy,2-methoxybenzylidene)anabaseine (4OH-GTS-21), an α7-selective agonist, is unaffected by mutation of Tyr188 to Phe, whereas ACh potency is drastically reduced in the mutant α7 receptor. The effect of the homologous mutation was

This work was supported by the National Institutes of Health National Institute of General Medical Sciences [Grant GM57481].
Article, publication date, and citation information can be found at http://jpet.aspetjournals.org.
doi:10.1124/jpet.109.151225.

ABBREVIATIONS: ACh, acetylcholine; LBD, ligand-binding domain; nAChR, nicotinic acetylcholine receptor; 4OH-GTS-21, 3-(4-hydroxy,2-methoxybenzylidene)anabaseine; AChBP, acetylcholine binding protein; AR-R17779, (−)-spiro[1-azabicyclo(2.2.2)octane-3,5′-oxazolidin-2′-one]; PDB, Protein Data Bank; PNU-120596, 1-(5-chloro-2,4-dimethoxy-phenyl)-3-(5-methyl-isoxanol-3-yl)-urea.

qualitatively different in heteromeric α4β2 receptors. Although ACh potency was unaffected by the α4Y195F (previously reported as α4Y190F) mutation, the efficacy of 4OH-GTS-21 was increased at least 200-fold in α4Y195Fβ2 receptors relative to wild type (Horenstein et al., 2007). These findings suggest that the assumption that all conserved residues play comparable roles in all receptor subtypes may be invalid and have led us to hypothesize that other conserved residues within the aromatic pocket may act as metaphorical pivots or fulcra that confer unique pharmacological properties to different receptor subtypes rather than as structural pillars, which play universal roles in all receptors in which they are conserved.

Seventeen known genes (α1–10, β1–4, δ, γ, and ε) are translated into membrane-spanning proteins that may form nAChR subunits and can assemble into a large variety of pentameric complexes that display distinct pharmacology, physiologic localization, and functionality (Dani and Bertrand, 2007). The LBD is localized at the interface of two subunits, and Trp55 and Trp149 (α7 numbering) are found on opposing sides of this interface. In heteromeric receptors such as α4β2 and muscle-type receptors, Trp57 is found on the non-α subunit (complementary face), whereas Trp154 (α4 numbering) is found on the α subunit (primary face) contributing to the binding site. As might be expected, the only subunits in which α7 Trp55 and β2 Trp57 are not conserved are subunits that do not form the complementary face, whereas the only subunits in which α7 Trp149 and α4 Trp154 are not conserved are subunits that do not contribute to the primary face of an agonist binding site (Fig. 1A). These tryptophans are both found in α subunits that can form homomeric receptors (α7–α10) because these α subunits contribute to both the primary and complementary faces of binding sites in the homomeric receptor (Kalamida et al., 2007). The crystal structure of acetylcholine binding protein (AChBP) isolated from *Lymnaea stagnalis*, which is homologous to the extracellular domain of a homomeric receptor (Brejc et al., 2001), suggests that the indole ring of the Trp at position 149 (human α7 numbering) is positioned vertically, deeper, and slightly higher in the binding pocket than Trp55, which is positioned horizontally at the mouth of the aromatic pocket (Fig. 1B).

In this study, we use site-directed mutagenesis and heterologous expression in *Xenopus laevis* oocytes to investigate the functional significance of α4 Trp154, β2 Trp57, α7 Trp55, and α7 Trp149 for the activation of homomeric and heteromeric neuronal nAChR by ACh and the structurally diverse α7-selective agonists choline, 4OH-GTS-21, and AR-R17779. Our data suggest that nAChR are probably activated in different manners by structurally distinct agonists and provide insight regarding the selective activation of nAChR subtypes.

Materials and Methods

cDNA Clones. Human nAChR receptor clones were obtained from Dr. Jon Lindstrom (University of Pennsylvania, Philadelphia, PA). The RIC-3 clone was obtained from Dr. Millet Treinin (Hebrew University, Jerusalem, Israel).

Site-Directed Mutants. Mutations of selected amino acids were introduced using the QuikChange kit from Stratagene (La Jolla, CA) according to the manufacturer's instructions. Sequences were confirmed with automated fluorescent sequencing at the University of Florida core facility.

Preparation of RNA. Subsequent to linearization and purification of cloned cDNAs, RNA transcripts were prepared in vitro using the appropriate mMessage mMachine kit from Ambion (Austin TX).

Expression in *X. laevis* Oocytes. Mature (>9 cm) female *X. laevis* African frogs (Nasco, Ft. Atkinson, WI) were used as a source of oocytes. Before surgery, the frogs were anesthetized by placing them in a 1.5 g/l solution of tricaine methanesulfonate for 30 min. Oocytes were removed from an incision made in the abdomen.

Harvested oocytes were treated with 1.25 mg/ml collagenase (Worthington Biochemicals, Freehold, NJ) for 2 h at room temperature in calcium-free Barth's solution (88 mM NaCl, 1 mM KCl, 2.38 mM $NaHCO_3$, 0.82 mM $MgSO_4$, 15 mM HEPES, pH 7.6, 12 mg/l tetracycline) to remove the follicular layer. Stage 5 oocytes were isolated and injected with 50 nl (5–20 ng) of each subunit cRNA. Recordings were normally conducted 2 to 5 days after injection, although for some mutants, longer periods of incubation (up to 8–10 days) were required to obtain measurable currents. Wild-type and mutant α7 receptors were routinely coinjected with the cDNA for human RIC-3, an accessory protein that improves and accelerates α7 expression (Halevi et al., 2003) without affecting the pharmacological properties of the receptors. α4β2 Receptors were injected at an α/β ratio of 1:1. Note that the injection of α4 and β2 subunits into the oocytes at a ratio of 1:1 results in a mixture of $(\alpha4)_2(b2)_3$ and $(\alpha4)_3(b2)_2$ stoichiometries (Kuryatov et al., 2008).

Electrophysiology. Experiments were conducted using OpusXpress6000A (Molecular Devices, Sunnyvale, CA). OpusXpress is an integrated system that provides automated impalement and voltage clamp of up to eight oocytes in parallel. Both the voltage and current electrodes were filled with 3 M KCl. The oocytes were clamped at a holding potential of −60 mV. Data were collected at 50 Hz and filtered at 20 Hz. The oocytes were bath-perfused with Ringer's solution (115 mM NaCl, 2.5 mM KCl, 1.8 mM $CaCl_2$, 10 mM HEPES, 1 μM atropine, pH 7.2). Agonist solutions were delivered from a 96-well plate using disposable tips. Flow rates were set at 2 ml/min for α7 and 4 ml/min for α4β2. Drug applications were 12 s for α7 and 6 s for α4β2 and usually alternated between ACh controls and test solutions of ACh or other experimental agonists at varying concentrations.

Chemicals. 4OH-GTS-21 was obtained from Taiho (Tokyo, Japan). AR-R17779 was provided by Critical Therapeutics, Inc. (Lexington MA). Other chemicals were purchased from Sigma-Aldrich (St. Louis, MO). Fresh acetylcholine stock solutions were made daily in Ringer's solution.

Molecular Modeling and Sequence Alignment. The molecular graphic of AChBP (Fig. 1B, PDB identification no. 1i9B; Brejc et al., 2001) was produced using the University of California San Francisco Chimera package from the Resource for Biocomputing, Visualization and Informatics at the University of California, San Francisco (Pettersen et al., 2004). Sequence alignments were generated using ClustalW (http://www.ebi.ac.uk/Tools/clustalw2/index.html) (Higgins et al., 1996). Homology modeling utilized the Swiss-Model Server (http://swissmodel.expasy.org) (Schwede et al., 2003; Kopp and Schwede, 2004; Arnold et al., 2006). In brief, the template for both human α7 and α4β2 nAChR dimer models was the crystal structure for AChBP in complex with cocaine (2PGZ; Hansen and Taylor, 2007). Cocaine has been shown previously to be a core structure that can be modified to form the α7-selective partial agonist cocaine methiodide (Francis et al., 2001). The 2PGZ structure was chosen because the binding of cocaine positions the C-loop in a way that is consistent with the accommodation of α7-selective agonists that are bulkier than ACh, such as cocaine methiodide, tropanes, quinuclidines, and benzylidene anabaseine compounds. Note that 2PGZ is the wild-type AChBP structure, containing the C-loop disulfide and all other conserved elements of the LBD. ClustalW sequence alignments were used between the AChBP sequence and human α7, α4, or β2 nAChR sequences. The resulting monomer models were then fit to the coordinates of an AChBP dimer to produce $\alpha7_2$ and α4β2 dimer models. Side chains experiencing clashes at the interface

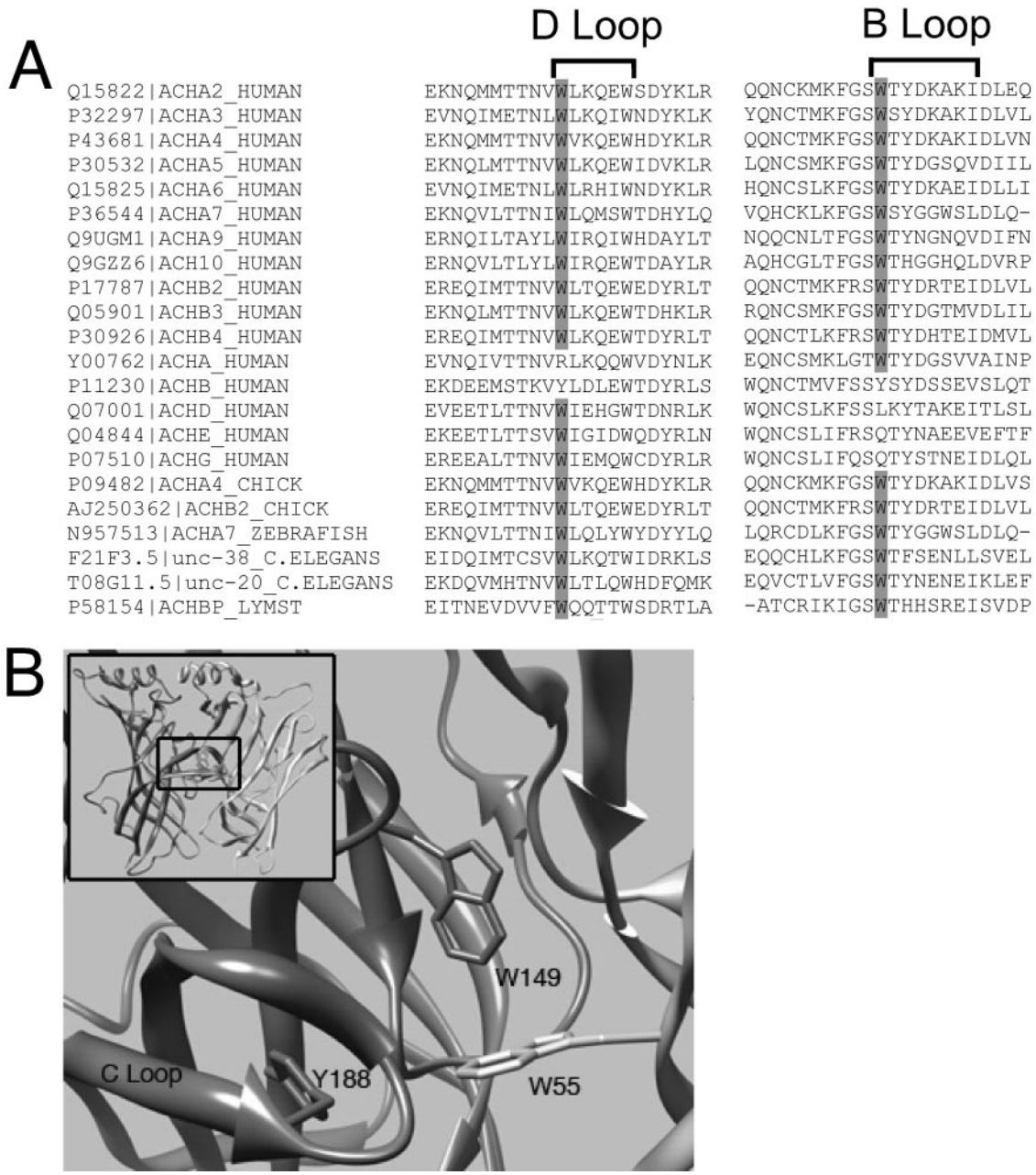

Fig. 1. Multiple sequence alignment and hypothetical localization of α4 Trp154, β2 Trp57, α7 Trp55, and α7 Trp149. A, multiple sequence alignment of human nAChR sequences with sample sequences from chick, *C. elegans*, and zebrafish show great conservation of both Trp residues throughout the nicotinic family and many species. unc-38 and unc-20 from *C. elegans* encode α and non-α subunits, respectively (http://www.wormbase.org). It is curious that these Ws are also conserved in the α5 and β3 subunits, which have been proposed to occupy the accessory subunit position and not contribute directly to the agonist binding domain (Gotti et al., 2006). B, close-up of the LBD from the crystal structure of AChBP isolated from *L. stagnalis* (PDB no. 1i9b). Numbering of residues correspond to human α7 numbering.

were identified and optimized using side-chain conformational searching and the GROMOS96 force field within the Swiss-PDBviewer (version 4.01). Modeling of 4OH-GTS-21 bound in the LBD of α7 or α4β2 models was performed with DOCK6.1 (Moustakas et al., 2006).

Experimental Protocols and Data Analysis. Responses of α4β2 wild-type and mutant receptors are reported as peak currents, and responses of α7 wild-type and mutant receptors are calculated as net charge (Papke and Porter Papke, 2002) because peak currents inaccurately report the agonist concentration dependence of α7-mediated responses (Papke and Thinschmidt, 1998).

Comparison of Functional Expression between Mutant and Wild-Type Receptors. ACh-induced maximal responses for mutant receptors compared with wild-type receptors were calculated by averaging responses to the same concentration of ACh on both wild-type and mutant receptors on the same day, using the same batch of oocytes that had been injected with equal amounts of RNA on the same day. Such precautions are necessary to accurately determine maximal responses relative to wild-type receptors because of biological variability inherent within oocytes harvested from different frogs. For example, differences in the mediators of metabolic processes (kinases, phosphatases, cyclic nucleotides, etc.) and/or hormonal regulation between individual frogs could affect rates of protein synthesis or intracellular signaling cascades leading to varied phosphorylation states among the expressed receptors. ACh tests were 300 μM for α7 wild-type and α7 Trp55 mutants. α7W55Y was

also tested with 30 μM ACh, and the nonresponsive mutants α7W55S and α7W55T were also tested with 3 mM ACh. ACh tests were 100 μM and 1 mM for α4β2 wild-type and α4β2 Trp57 mutants. ACh tests were 300 μM and 1 mM for α7 wild-type and α7 Trp149 mutants and 30 μM and 1 mM for α4β2 wild-type and α4W154β2 mutants. Four to 18 oocytes were tested from each group, with on average $n = 7$. The test ACh responses were then normalized to the expected ACh maximum for each receptor type as determined by full ACh concentration response studies done separately.

Concentration-Response Relationships. Each oocyte received two initial control applications of ACh followed by the experimental drug application and a subsequent control application of ACh. For experiments with α7 wild-type and mutant receptors, the control ACh concentration was 300 μM, with the exception that 30 μM ACh was used as the control for α7W55Y because this mutant could not be activated repeatedly by 300 μM ACh without rundown, hypothetically, because of accumulated desensitization; and choline and ACh curves for α7W55G were done using 1 mM ACh as a control because results were overly variable when 300 μM ACh was used as the control, presumably, because of the low potency of ACh for this mutant. For experiments with α4β2 wild-type receptors and α4β2 Trp57 mutants, control applications of ACh were 30 μM, and for experiments with α4W149β2 mutants, control ACh applications were 100 μM ACh. Responses to experimental drug applications were calculated relative to the preceding ACh control responses to normalize the data, compensating for the varying levels of channel expression among the oocytes, and were subsequently normalized to the ACh maximal response for each receptor type, determined from separate ACh concentration-response experiments.

Mean values and S.E.M. values were calculated from the normalized responses of at least four oocytes (average, seven) for each experimental concentration. For concentration-response relations, data were plotted using Kaleidagraph 3.52 (Synergy Software, Reading, PA), and curves were generated from the Hill equation: response = $(I_{max}[\text{agonist}]^n)/([\text{agonist}]^n + (EC_{50})^n)$, where I_{max} denotes the maximal response for a particular agonist/subunit combination, and n represents the Hill coefficient. I_{max}, n, and the EC_{50} were all unconstrained for the fitting procedures except in the case of the ACh concentration-response curves. Because ACh is our reference full agonist, those data were normalized to the observed ACh maximum, and the I_{max} of the curve fits were constrained to equal 1. Although some α4β2 concentration-response curves were not ideally fit by the single-site Hill equation, presumably, because α4β2 receptors expressed from RNA injected at an α4/β2 ratio of 1:1 resulted in α4β2 receptors of mixed stoichiometry (Kuryatov et al., 2008), in most cases, the single-site Hill equation provided better concentration-response curve fits than the double-site Hill equation, so for consistency, single-site fits were generated for all α4β2 data sets.

Results

Mutation of Trp55 or Trp57 of α7 and α4β2 Receptors, Respectively, Alters the Pharmacology and Regulates the Selectivity of 4OH-GTS-21. We anticipated two general types of effects that would result from mutations in the nAChR LBD; first, that there would be changes in the ability of ACh to promote channel activation; and second, that there would be differences in the relative efficacy of α7-selective agonists compared with ACh.

Because our primary goal was to test the hypothesis that α7-selective agonists may promote activation through mechanisms that are distinct from the activation mechanism invoked by ACh, changes in relative efficacy were of particular interest. Although measurements of relative efficacy are readily obtainable from macroscopic currents as long as a reliable reference by which to measure efficacy is employed, effects of the first type, on the absolute ability of ACh to promote activation, are relatively difficult to measure from macroscopic currents because decreases in ACh-evoked responses may result from either decreased ACh activity or decreased receptor expression. An obstacle in this study for the application of traditional measurements of receptor expression, such as radioligand binding assays, is that mutations of highly conserved LBD residues are arguably equally likely to affect ligand binding as receptor activation, potentially rendering results of binding experiments uninterpretable.

Absolute Efficacy of ACh. With this limitation in mind, we estimated the effects of our mutations on the absolute effectiveness of ACh to promote channel activation based on comparisons of the maximal ACh-induced currents in our mutants to the maximal ACh-induced currents in wild-type receptors that were injected the same day from the same harvest of oocytes with RNA of comparable amount and quality, as confirmed on denaturing gels, in combination with concentration-response curves for ACh. The estimates should be accurate to the degree that the LBD mutation had a greater effect on ACh activation than on net receptor expression. These measurements of maximal ACh-induced currents then formed the basis from which efficacies of choline, 4OH-GTS-21, and AR-R17779, relative to ACh responses in wild-type and mutant receptors, were subsequently determined. Choline and AR-R17779 are considered full agonists of α7, activating α7 as efficaciously as ACh, whereas 4OH-GTS-21 is an α7-selective partial agonist. None of these drugs produce significant currents in α4β2 receptors (Fig. 2).

Calculated ACh maximal responses for α7W55A and α7W55G mutants were approximately 2.5 times larger than for wild type, the α7 Trp55 to Val mutant maximal responses were approximately equal to wild type, and α7W55Y and α7W55F had ACh maximal net-charge responses approximately one half as large as wild-type α7 (Fig. 3A). It has been reported previously (Gay et al., 2008) that the W55A mutant of rat α7 showed a reduced decay rate in macroscopic currents, which might account for our observed increase in net charge compared with wild-type α7. However, our data indicate that, similar to wild-type α7, the human W55A and W55G mutants show typical concentration-dependent desensitization, such that the net charge of the ACh responses reaches a maximal value at relatively low concentrations of agonist, whereas peak currents show a higher apparent EC_{50} (data not shown).

Homologous mutations were made in β2; wild-type and β2 mutant subunits were coexpressed (1:1) with α4. As with the α7 Trp55 mutants, the α4β2W57A, α4β2W57G, α4β2W57V, α4β2W57Y, and α4β2W57F mutants gave functional responses to ACh, and α4β2W57R, α4β2W57S, and α4β2W57T mutants did not (Fig. 3, B and D). However, none of the α4β2 mutant peak currents was as large as the wild-type responses. The calculated maximal ACh responses of the functional mutants were on average approximately 1/10 of the wild-type calculated maximal ACh peak response (Fig. 3C). Nonetheless, the ACh potencies were greater for some of the α4β2 Trp57 mutants than for the wild type.

Relative Efficacy of α7-Selective Agonists Compared with ACh. The mutation of α7 Trp55 to the nonaromatic amino acids Ala, Gly, and Val resulted in reduced potencies for all the agonists tested (Fig. 4, A–C; Table 1). Although

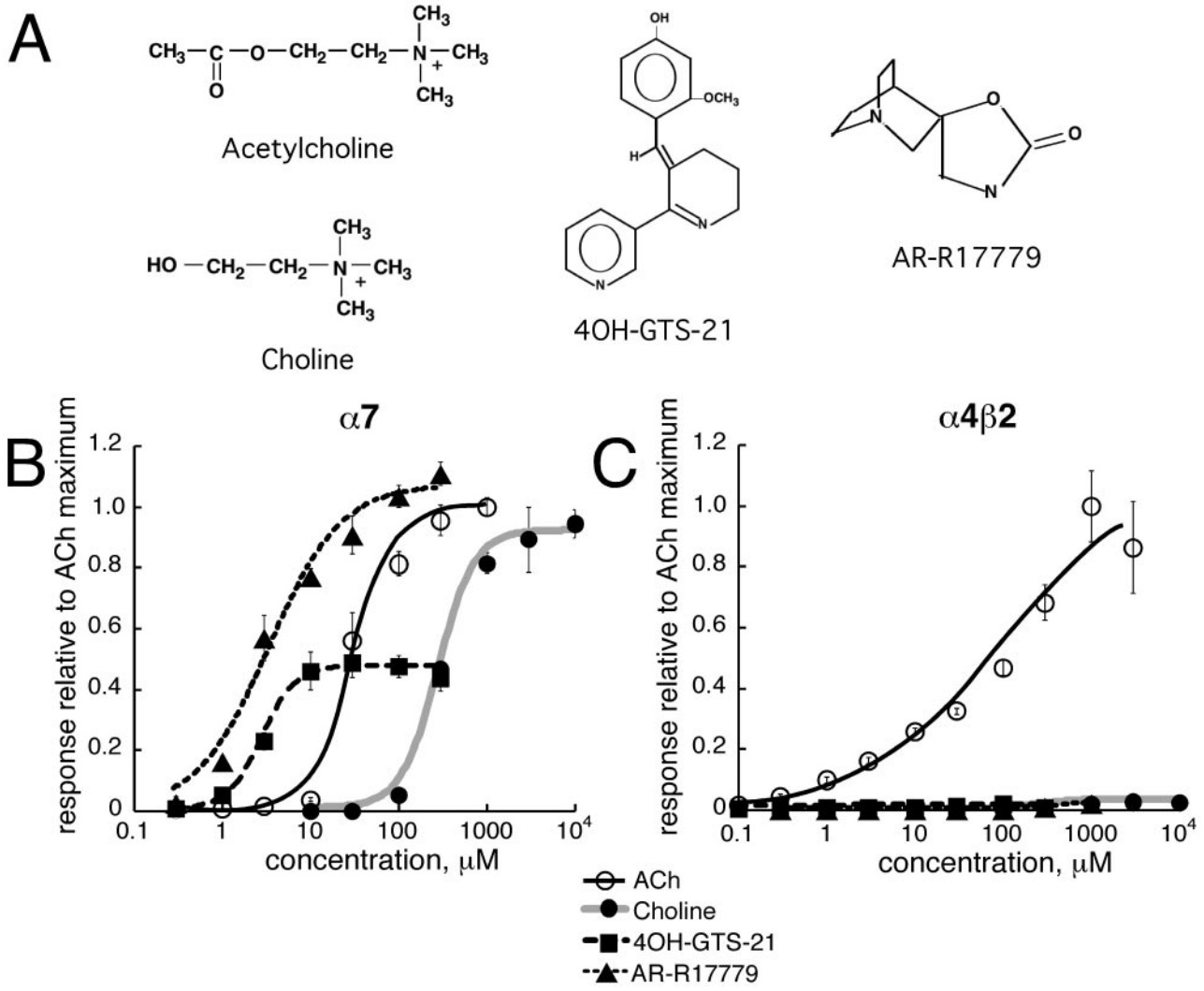

Fig. 2. Concentration-response relationships of wild-type α7 and α4β2 receptors to ACh, choline, 4OH-GTS-21, and AR-R17779. A, chemical structures of the agonists used in this study. B, net-charge responses of wild-type α7. C, peak responses of wild-type α4β2. Each data point represents the mean (±S.E.M.) of at least four oocytes. For consistency, the single-site Hill equation was used to fit the α4β2 curve because the single-site model provided the best fit for most α4β2 mutants in this study. There were no significant differences in χ^2 or R values between fits by the single-site or biphasic models.

mutation of α7 Trp55 to Gly produced a decrease in the potency of ACh, choline, and AR-R17779 (22-, 14-, and >92-fold increases in EC_{50} values, respectively, Table 1), maximal responses to these agonists were larger than those of wild-type receptors. Maximal ACh responses of α7W55G mutants were approximately 2.5-fold higher than maximal ACh responses in wild-type receptors. Relative to the maximal ACh-induced currents in wild-type and mutant receptors, choline efficacy was increased (Fig. 4B). Although the 10 mM choline responses were significantly larger than the 1 mM ACh responses recorded in the same cells ($n = 10, p < 0.05$), because of the low potency of choline for the W55G mutant, we were unable to achieve a saturating I_{max} for choline in the concentration range tested (up to 10 mM). In contrast to the results seen with ACh and choline, α7W55G receptors did not produce measurable responses to 4OH-GTS-21 in the concentration range tested. Mutation of α7 Trp55 to Ala or Val likewise resulted in decreased agonist potencies, although not as greatly as with the mutation to Gly (Fig. 4, A and C; Table 1). 4OH-GTS-21 activated the α7W55V mutant as efficaciously as ACh (Fig. 4C). The relatively conservative mutation of Trp55 to Tyr or Phe did not significantly affect ACh potency because EC_{50} values remained near 30 μM. However, the potencies of choline, 4OH-GTS-21, and AR-R17779 were all altered by these mutations (Table 1). Mutation of Trp55 to Phe caused the EC_{50} of 4OH-GTS-21 to increase 6-fold (Fig. 4D), and mutation of Trp55 to Tyr yielded mutant α7 receptors that did not give detectable responses to 4OH-GTS-21.

The low efficacy of 4OH-GTS-21 for the W55G and W55Y α7 mutants seems to be, at least in part, related to desensitization and/or channel block by 4OH-GTS-21. When 100 μM 4OH-GTS-21 was coapplied with ACh to the W55G and W55Y mutant receptors, responses were significantly decreased compared with responses to ACh applied alone ($p < 0.05$, data not shown). We have previously characterized a similar type of residual inhibition/desensitization in wild-type α7 receptors (Papke et al., 2009) and have shown that it can represent a form of stabilized desensitization that is reversed by the application of the type 2 positive allosteric modulator PNU-120596. Although 4OH-GTS-21 was rela-

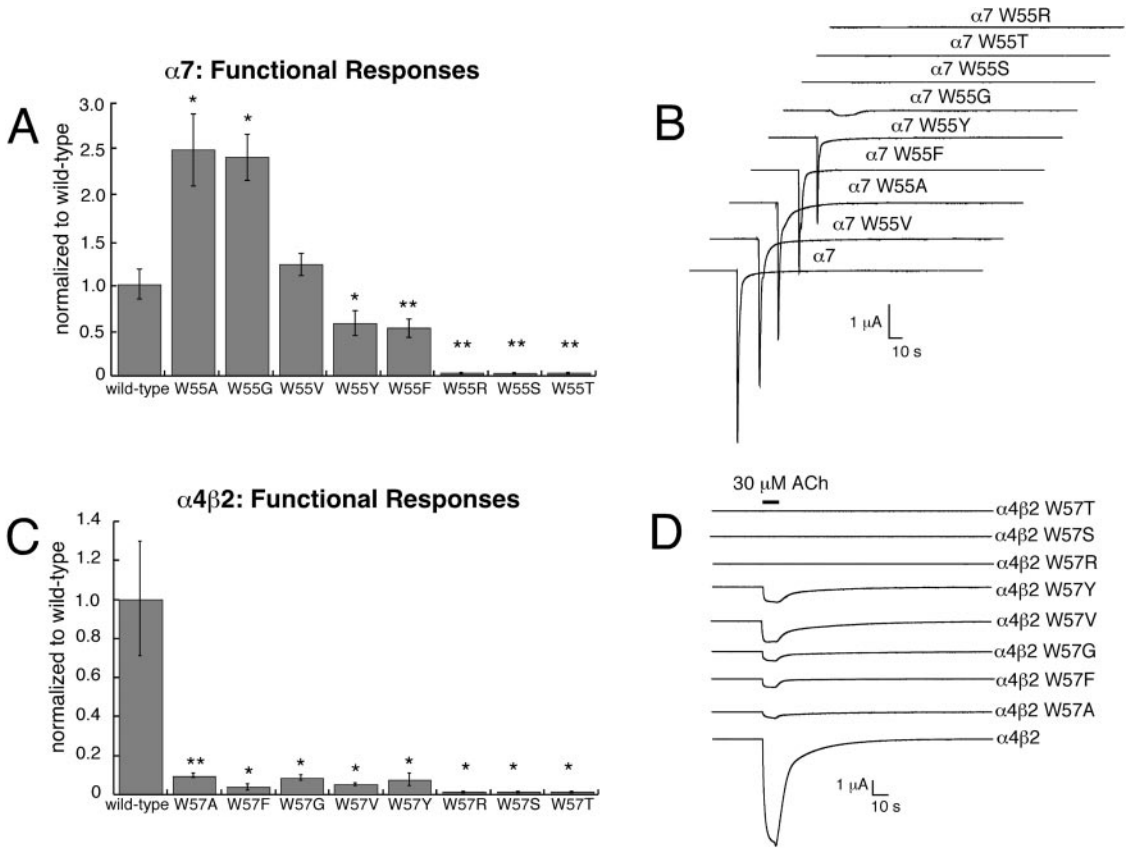

Fig. 3. Functional responses of human α7 Trp55 and human α4β2 Trp57 mutant receptors relative to ACh-induced maximal responses in wild-type. A, maximal net-charge responses of α7 Trp55 mutant receptors relative to the ACh-induced maximal net-charge response in wild-type α7, represented as a value of 1. * and **, statistically significant differences in maximal functional responses between wild-type and mutant receptors with $p < 0.05$ and $p < 0.01$, respectively. B, representative data traces of responses by α7 wild-type and α7 Trp55 mutants to 300 μM ACh. C, maximal peak responses of α4β2 Trp57 mutants relative to the ACh-induced maximal peak response in wild-type α4β2, represented as a value of 1. * and **, $p < 0.05$ and $p < 0.01$, respectively. D, representative data traces of α4β2 Trp57 mutant receptors in response to 30 μM ACh. Maximal responses for mutant receptors compared with wild type were calculated by averaging responses (±S.E.M.) of at least four oocytes to the same concentration of ACh on both wild-type and mutant receptors injected the same day, with the same amount of RNA from the same harvest of oocytes. Averaged responses were divided by the percentage of ACh maximum for that concentration on a fitted ACh concentration-response curve to find the maximal theoretical response and then divided by the calculated maximal response for the wild-type receptor for the comparison.

tively ineffective at activating α7 W55G and W55Y mutant receptors, large currents occurred when 4OH-GTS-21 was applied with PNU-120596 (data not shown). These observations suggest that 4OH-GTS-21 has access to the binding site in the α7 Trp55 mutants and promotes PNU-120596-sensitive desensitization much more effectively than activation.

Homologous mutations in the LBD of α4β2 receptors (β2 Trp57) produced qualitatively different results from the mutations made in α7. Mutation to Gly greatly reduced ACh potency in α7 receptors but increased ACh potency in α4β2W57G mutants. Mutation of Trp55 to Tyr in α7 receptors did not affect ACh potency, but ACh was twice as potent for α4β2W57Y mutants as for wild-type receptors. ACh also had greater potency for α4β2W57F than for wild-type α4β2. However, ACh had significantly lower potency for α4β2W57A than for wild-type α4β2. Neither choline nor AR-R17779 activated any of the α4β2 receptors (Fig. 5, A–E; Table 1). However, 4OH-GTS-21 did activate four of the α4β2 Trp57 mutants and provided the most interesting differences among these Trp55 and Trp57 mutants of the α7-selective agonists tested. Note that maximal ACh responses of the α4β2 mutants were approximately 1/10 of the maximal responses in wild-type receptors. Although it is true that a selective compromise in ACh-mediated activation would have the tendency to make the relative efficacies of the experimental agonists appear increased, that effect would be manifested in the results of all experimental agonists normalized to the ACh responses. However, our data indicate that the increase in the relative efficacy of 4OH-GTS-21 is many times larger than that of either choline or AR-R17779, which were both immeasurable because currents induced by these drugs were too small to be determined. Therefore, the increased activation of α4β2 mutants by 4OH-GTS-21 is likely to represent a true potentiation of an activation mechanism potentially unique to 4OH-GTS-21 and related compounds. 4OH-GTS-21 activated wild-type α4β2 only approximately 2% and wild-type α7 46% as well as ACh (Fig. 2, B and C). 4OH-GTS-21 activated α4β2W57A, α4β2W57G, α4β2W57F, and α4β2W57Y but not α4β2W57V, α4β2W57R, α4β2W57S, or α4β2W57T mutant receptors. Interestingly, 4OH-GTS-21 activated α7W55V mutants, and ACh did as well. 4OH-GTS-21 activated α4β2W57A, α4β2W57F, and α4β2W57G to 60 to 70% of their ACh maxima, with lowest potency in α4β2W57A and highest potency in α4β2W57Y and α4β2W57F mutants. It is important that peak responses of α4β2W57Y to 4OH-GTS-21 were 2.5-fold greater than for ACh, whereas the homologous mutation in α7 decreased the relative efficacy of 4OH-GTS-21 greatly.

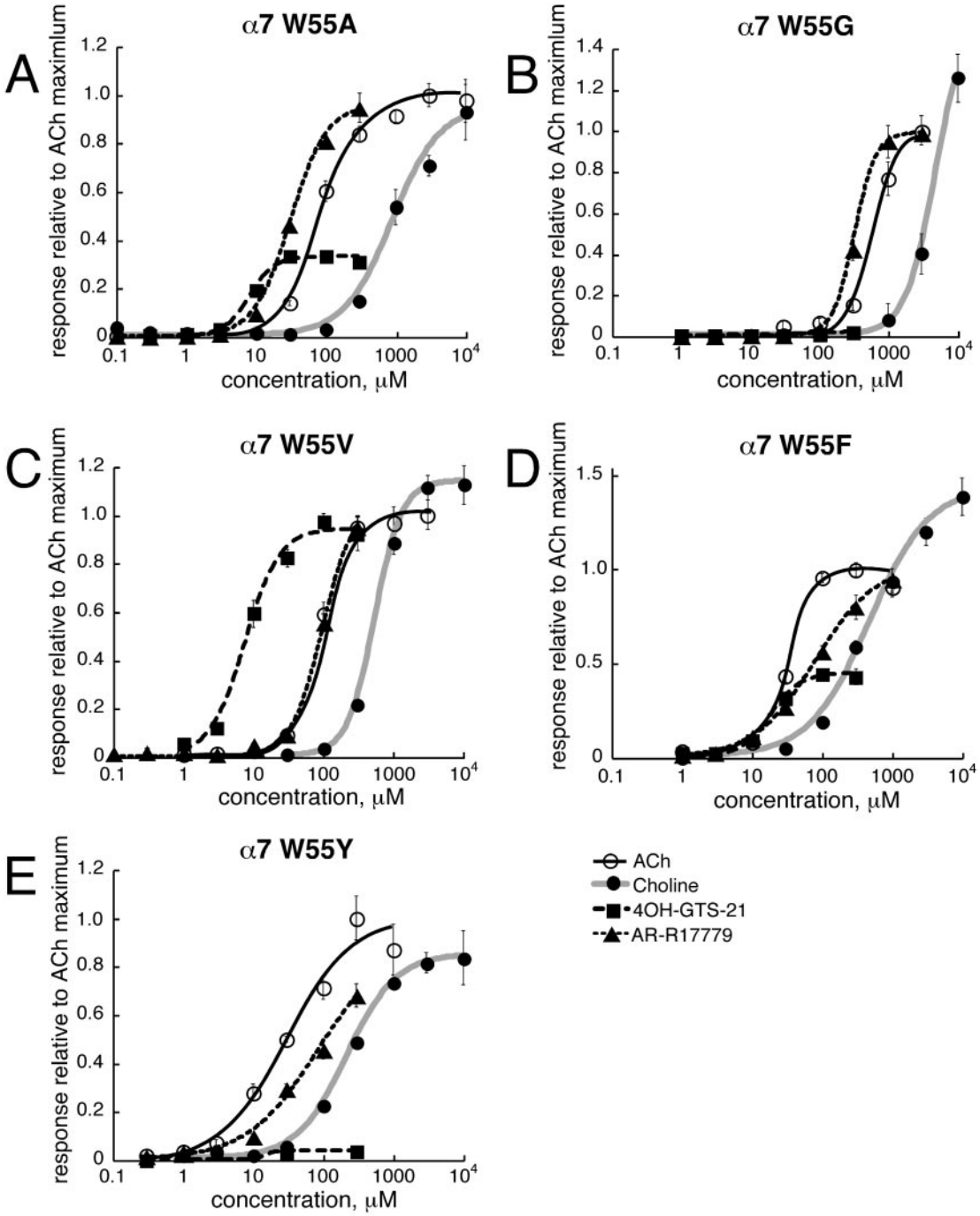

Fig. 4. Concentration-response relationship of α7 Trp55 mutant receptors to ACh, choline, 4OH-GTS-21, and AR-R17779. A, net-charge responses of α7W55A mutants. B, net-charge responses of α7W55G mutants. Note the low efficacy of 4OH-GTS-21. C, net-charge responses of α7W55V mutants. D, net-charge responses of α7W55F mutants. E, net-charge responses of α7W55Y mutants. Note the low efficacy of 4OH-GTS-21. Responses of wild-type α7 are presented in Fig. 2B. Data were measured relative to control ACh responses and then expressed relative to the maximal ACh response for each particular receptor type. Each point represents the mean (±S.E.M.) of at least four oocytes.

Mutation of Trp149 in Both α7 and α4β2 Receptors Reduced Receptor Activation by Both ACh and α7-Selective Agonists. Responses of α7 Trp149 mutant receptors were significantly lower ($p < 0.05$) than those of wild-type α7 receptors recorded the same number of days after injection. It is somewhat surprising that the relatively conservative mutations of α7 Trp149 to Phe or Tyr disrupted receptor responses to ACh to levels below the limits of detection, whereas the nonconservative mutations to Ala or Gly yielded receptors that were capable of producing measurable ACh-induced currents. The α7W149V mutant receptors were also nonresponsive to ACh (Fig. 6A). Of the mutant receptors that were nonresponsive to ACh, none was able to produce recordable currents in response to choline, 4OH-GTS-21, or AR-R17779, with the exception of α7W149F mutants, which reproducibly yielded small but measurable currents in response to choline (data not shown). The fact that only two of the five α7 Trp149 mutants were sufficiently functional for

TABLE 1
EC_{50} and I_{max} values of ACh, choline, 4OH-GTS-21, and AR-R17779 in wild-type and mutant α7 and α4β2 receptors

Drug	Receptor	EC_{50} ± S.E.M.	I_{max} ± S.E.M. Relative to ACh Maximum	I_{max} ± S.E.M. Relative to Wild-Type ACh Maximum
ACh	α7	31 ± 4	1	1
	α7W55A	85 ± 6	1	2.5 ± 0.4
	α7W55F	33 ± 3	1	0.5 ± 0.1
	α7W55G	602 ± 35	1	2.4 ± 0.25
	α7W55V	84 ± 2.5	1	1.2 ± 0.1
	α7W55Y[¥]	30 ± 5	1	0.6 ± 0.2
	α7W149A	194 ± 10	1	0.15 ± 0.03
	α7W149G	400 ± 19	1	0.17 ± 0.03
	α4β2	76 ± 20	1	1
	α4β2W57A	468 ± 59	1	0.09 ± 0.01
	α4β2W57F	33 ± 4	1	0.04 ± 0.02
	α4β2W57G	47 ± 11	1	0.08 ± 0.02
	α4β2W57V	87 ± 10	1	0.05 ± 0.013
	α4β2W57Y	16 ± 2	1	0.08 ± 0.03
	α4W154A β2	526 ± 28	1	0.40 ± 0.04
	α4W154F β2	118 ± 6	1	0.39 ± 0.06
	α4W154Y β2	81 ± 3	1	0.04 ± 0.00
Choline	α7	304 ± 21	0.90 ± 0.02	0.90 ± 0.02
	α7W55A	950 ± 210	0.95 ± 0.05	2.3 ± 0.1
	α7W55F	500 ± 72	1.4 ± 0.07	0.73 ± 0.04
	α7W55G	>5000	1.3 ± 0.12	>1.5
	α7W55V	570 ± 12	1.1 ± 0.01	1.4 ± 0.1
	α7W55Y	228 ± 13	0.84 ± 0.01	0.48 ± 0.01
	α7W149A	2490 ± 130	0.89 ± 0.03	0.13 ± 0.01
	α7W149G	6870 ± 1440	0.61 ± 0.07	0.10 ± 0.02
4OH-GTS-21	α7	3.0 ± 0.3	0.46 ± 0.01	0.46 ± 0.01
	α7W55A	8.4 ± 0.7	0.33 ± 0.01	0.82 ± 0.02
	α7W55F	19 ± 2	0.45 ± 0.02	0.23 ± 0.01
	α7W55G	N.A.*	N.A.*	N.A.*
	α7W55V	7.8 ± 0.8	0.94 ± 0.03	0.54 ± 0.02
	α7W55Y	N.A.*	N.A.*	N.A.*
	α7W149A	4.5 ± 1.4	0.28 ± 0.04	0.04 ± 0.01
	α7W149G	4.4 ± 0.5	0.76 ± 0.08	0.13 ± 0.02
	α4β2	N.A.*	0.01 ± 0.00	0.01 ± 0.005
	α4β2W57A	2.6 ± 0.3	0.71 ± 0.02	0.07 ± 0.01
	α4β2W57F	0.66 ± 0.22	0.62 ± 0.05	0.02 ± 0.002
	α4β2W57G	1.2 ± 0.2	0.74 ± 0.04	0.06 ± 0.01
	α4β2W57V	3.00 ± 0.14	0.07 ± 0.01	0.0035 ± 0.0005
	α4β2W57Y	0.65 ± 0.09	2.7 ± 0.1	0.19 ± 0.01
AR-R17779	α7	3.60 ± 0.73	1.05 ± 0.05	1.05 ± 0.05
	α7W55A	32.4 ± 1.7	0.96 ± 0.02	2.36 ± 0.05
	α7W55F	82.3 ± 2.5	1.02 ± 0.01	0.53 ± 0.01
	α7W55G	332 ± 2	0.99 ± 0.04	2.36 ± 0.10
	α7W55V	94 ± 6	1.05 ± 0.04	1.26 ± 0.05
	α7W55Y	87 ± 42	0.90 ± 0.16	0.51 ± 0.09
	α7W149A	120 ± 4	1.07 ± 0.14	0.16 ± 0.02
	α7W149G	506 ± 72	0.97 ± 0.09	0.17 ± 0.02

N.A., not available.
* Responses were below the limits of detection.
[†] The *n* values ranged from 4 to 18 and were, on average, 7.

use in this study suggests that mutation introduced at position 149 may interfere with receptor assembly or with conformational changes linked to channel opening. The mutations introduced at position 149 in α7 resulted in drastically reduced potencies of ACh, choline, and AR-R17779 (Table 1). Mutation of α7 Trp149 to Gly had profound effects on receptor activation, resulting in 13-, 20-, and 140-fold increases in EC_{50} values over those seen in wild-type receptors for ACh, choline, and AR-R17779, respectively. However, neither α7W149A nor α7W149G mutant receptors had significantly altered potency for 4OH-GTS-21 compared with wild type. Compared with the maximal response of ACh in wild-type receptors, the efficacy of choline fell 30%, and the efficacy of 4OH-GTS-21 rose 50% in α7W149G mutants (Fig. 6, C and D; Table 1).

α4W154β2 mutant receptors produced measurable ACh-induced currents when mutations to Ala, Phe, or Trp were introduced, whereas currents were undetectable when Gly was introduced at position 149, roughly the opposite of what was observed in α7 Trp149 mutants (Fig. 7, A and B). This observation is suggestive of intrinsic differences between the α7 and α4β2 LBDs. There was no functional expression of α4W154Gβ2 or α4W154Vβ2 mutant receptors detected; these mutants were also nonresponsive to choline, 4OH-GTS-21, and AR-R17779 (data not shown).

Mutation of α4 Trp154 to Ala resulted in a 7-fold increase in the EC_{50} for ACh, whereas mutations to Phe or Tyr did not greatly alter ACh potency compared with wild type. Of the α4W154β2 mutants tested, none responded to choline, AR-R17779, or 4OH-GTS-21 (Fig. 7, C and E).

In general, a loss of receptor function was observed as a result of any mutation introduced at the Trp149 position, at least for the agonists we tested and mutations we introduced. Taken together, these results suggest the Trp55 position may better tolerate mutation than Trp149 and, when mutated, allows for major alterations in the receptor

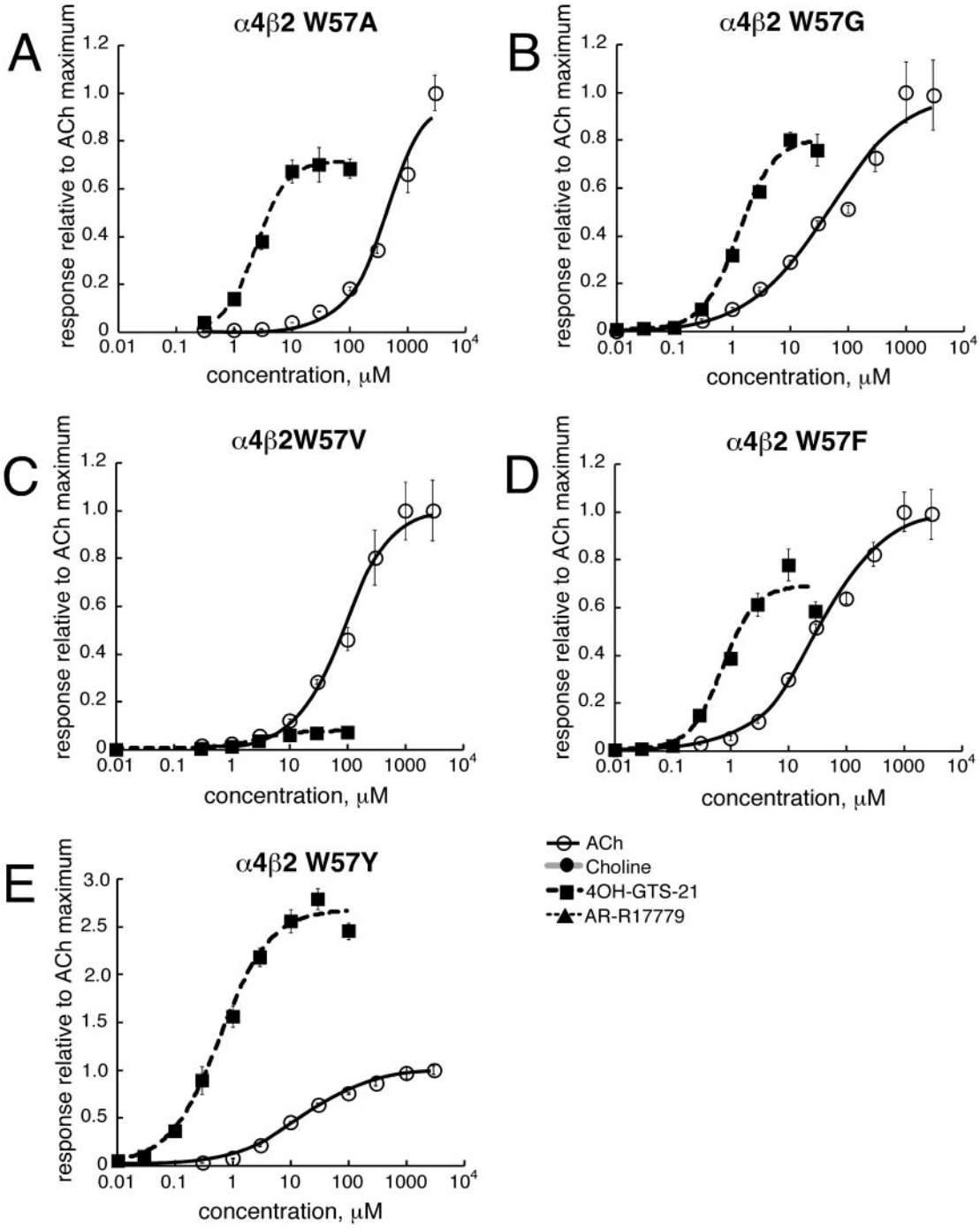

Fig. 5. Concentration-response relationships of α4β2 Trp57 mutants to ACh, choline, 4OH-GTS-21, and AR-R17779. A, peak responses of α4β2W57A mutant receptors. B, peak responses of α4β2W57G mutant receptors. C, peak responses of α4β2W57V mutant receptors. D, peak responses of α4β2W57F mutant receptors. E, peak responses of α4β2W57Y mutant receptors. Note that α4β2W57A, α4β2W57G, α4β2W57F, and α4β2W57Y mutants responded to 4OH-GTS-21. Responses to choline and AR-R17779 were below the limits of detection of all α4β2 receptors. Data were measured relative to control ACh responses and then expressed relative to the maximal ACh response for each particular receptor type. Each point represents the mean (±S.E.M.) of at least four oocytes. Peak responses by wild-type α4β2 are presented in Fig. 2C.

activation mechanisms, especially in regard to choline and 4OH-GTS-21.

Homology Modeling of the α7 and α4β2 Ligand Binding Domains with 4OH-GTS-21. Figure 8 presents views of 4OH-GTS-21 docked in the LBD of the human α7 and α4β2 receptors based on homology modeling. The viewer's perspective is from the extracellular side of the receptor, with the C loop and the cysteine disulfide in the lower left. Docking 4OH-GTS-21 into either the α7 or α4β2 receptor model produced very similar poses for the compound-receptor complex. One difference between these complexes is that Trp149 and Trp55 are in close communication in the α7 model but are not in the heteromeric receptor. The indole ring of Trp55 has a "flipped" conformation in the α4β2 model relative to the α7 model because the initially obtained model suffered from noncovalent interactions that were relieved by rotating the

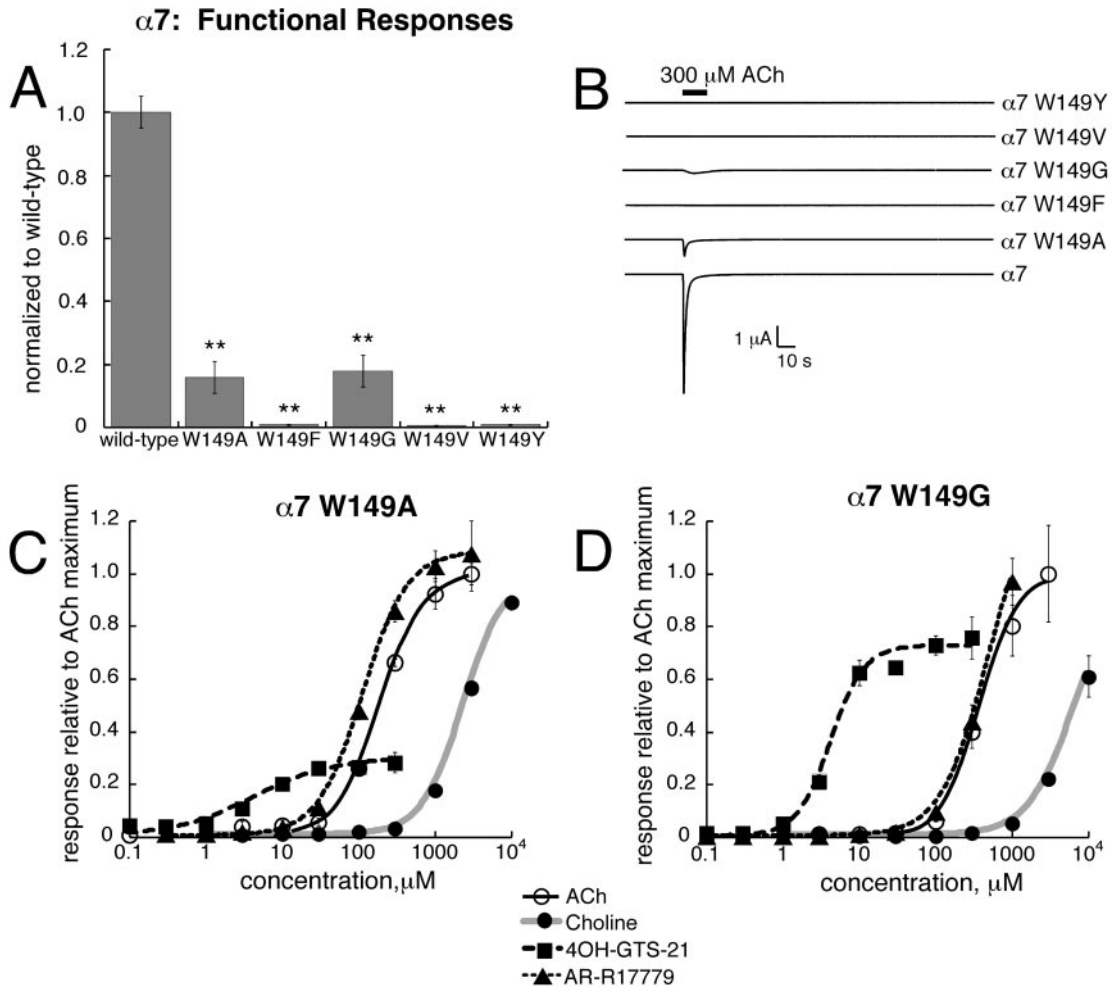

Fig. 6. Concentration-response relationships of α7 Trp149 mutants to ACh, choline, 4OH-GTS-21, and AR-R17779. A, maximal ACh-induced net-charge responses of α7 Trp149 mutants compared with maximal net-charge response of ACh in wild-type α7. **, $p < 0.01$. B, representative data traces of α7 Trp149 mutants in response to 300 μM ACh. C, net-charge responses of α7W149A mutant receptors. D, net-charge responses of α7W149G mutant receptors. Each data point represents the mean (±S.E.M.) of at least four oocytes. Responses of wild-type α7 to these agonists are presented in Fig. 2B.

Trp57 β-γ bond by approximately 180° before minimization. Another key difference observed between the poses for the two receptors was that docking 4OH-GTS-21 into the α4β2 receptor model resulted in a twist of the benzylidene double bond by approximately 50°, an unreasonable amount. None of the other low-energy poses identified placed the 4OH-GTS-21 in a similar location within the LBD.

Discussion

Numerous mutational studies of α7 Trp55 and α7 Trp149 (and homologous residues in other nAChR subtypes) and other conserved aromatic residues within the aromatic box of the nAChR LBD generally lead one to believe that mutation of conserved aromatic residues results in reduced receptor functionality. Building on evidence from a previous study, which showed that mutation of α7 Tyr188 does not necessarily knock down receptor functionality for all agonists, we investigated the functional significance of the conserved α7 Trp55, β2 Trp57, α7 Trp149, and α4 Trp154 residues.

Using unnatural amino acid substitutions in muscle-type nAChR at positions αTrp86, αTrp149, αTrp184, and γTrp55/δTrp57 with Trp derivatives containing various degrees of predicted cation interaction energies, αTrp149 has been shown to establish primary interactions with the quaternary ammonium group of acetylcholine (Zhong et al., 1998; Xiu et al., 2009). Structures of AChBP reveal either a charged nitrogen poised over the indole ring or hydrogen bonding interactions with ligands and the AChBP Trp143, homologous to human α7 Trp149 (Brejc et al., 2001; Celie et al., 2004; Hansen et al., 2005). Another implication of the data from Zhong et al. was that Trp55 may not directly stabilize the quaternary group of ACh through cation-π interactions, and the specific role of this residue in receptor activation remains an open question. In Torpedo receptors, mutation of γTrp55 to Leu reduced ACh affinity 7000-fold, whereas similar mutation of δ Trp57 resulted in only a 20-fold reduction. Double-mutant receptors (γW55L and δW57L) were reported to have reduced binding of many small agonists, including tetramethylammonium. Nicotine binding, however, was unaffected by the double-mutant receptors (Xie and Cohen, 2001). Trp55 was recently proposed to affect desensitization kinetics (Gay et al., 2008). However, results of this study are inconclusive because α7 currents were measured as peak responses (Papke and Porter Papke, 2002); mutation of Trp55 affected

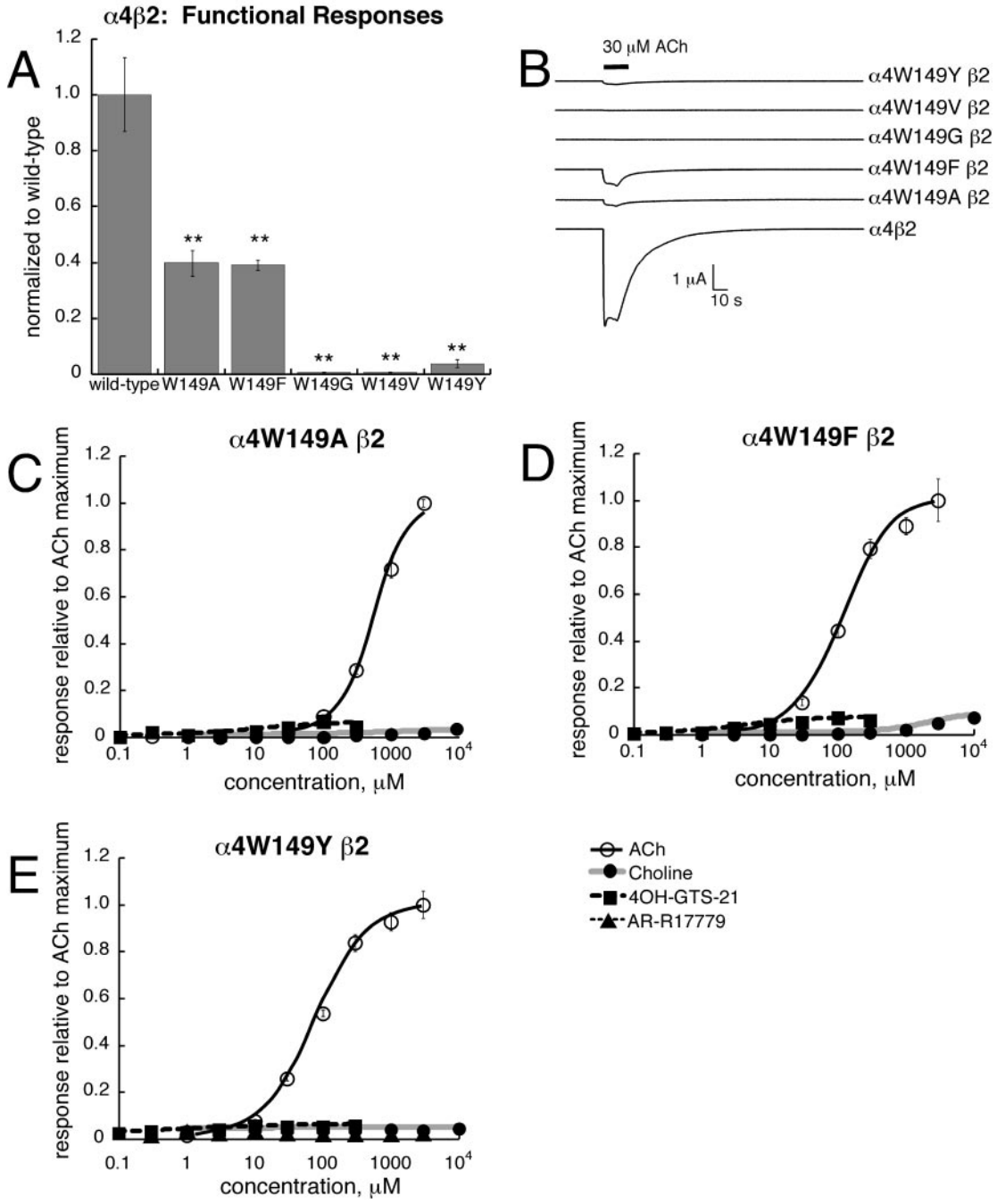

Fig. 7. Concentration-response relationships of α4W154β2 mutants to ACh, choline, 4OH-GTS-21, and AR-R17779. A, maximal ACh-induced peak responses of α7 Trp149 mutants compared with the maximal peak response of ACh in wild-type α7. **, $p < 0.01$. B, representative data traces of α4W154β2 mutants in response to 30 μM ACh. C, peak responses of α4W154Aβ2 mutants. D, peak responses of α4W154Fβ2 mutants. E, peak responses of α4W154Aβ2 mutants. Each data point represents the mean (±S.E.M.) of at least four oocytes. Peak responses by wild-type α4β2 are represented in Fig. 2C.

agonist potency, which in turn alters the response waveform (Papke, 2006); and macroscopic currents alone are insufficient to determine kinetics of desensitization.

Our data suggest that the conserved residues Trp149 and Trp55 have different functional significance in α7 nAChR, behaving as a pillar or as a fulcrum, respectively (Fig. 9). We apply the fulcrum metaphor to Trp55 and Tyr188 (α7 numbering) because mutation of these amino acids provides ligand and/or subtype-dependent changes in channel activation. Although the α7-agonist 4OH-GTS-21 lost efficacy in α7 Trp55 mutants relative to ACh, the same agonist gained efficacy, up to 300-fold compared with ACh in some α4β2 Trp57 and α4Y195Fβ2 mutants. The data from the current study suggest that Trp55 may be a critical residue for how 4OH-GTS-21 can either activate or fail to activate the gating mechanism. Perhaps the same ligand-residue interactions exist in both α7 and α4β2 nAChR subtypes but with different effects on activation, or perhaps the homologous residues form different ligand-residue interactions depending on the receptor subtype. For example, cation-π interactions may be

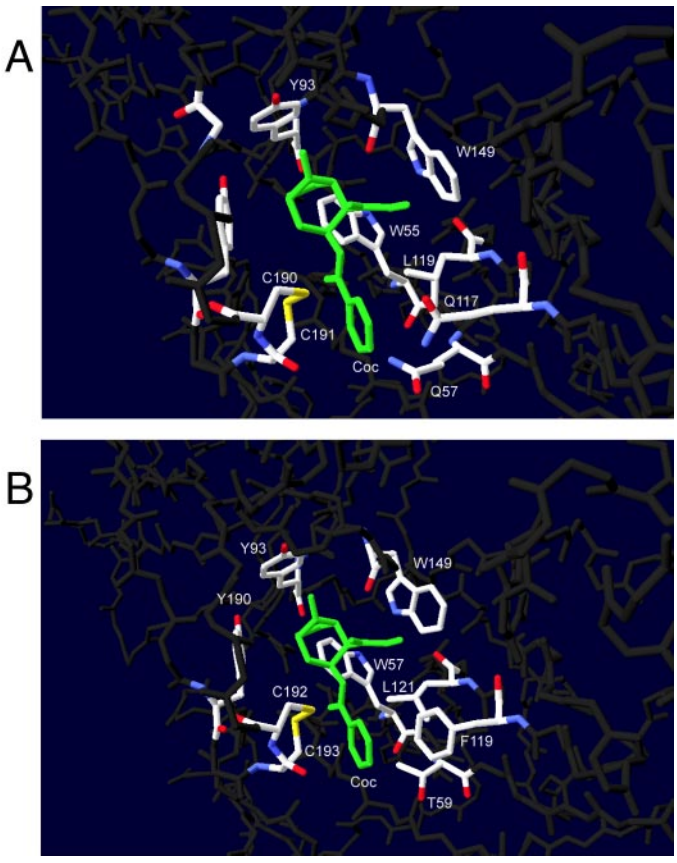

Fig. 8. LBDs for α7 and α4β2 nAChR homology models. A, α7 structure with the best pose obtained for docking the agonist 4OH-GTS-21 into the LBD. The two key tryptophan residues, Trp149 and Trp55, are labeled. B, α4β2 structure with a similar pose for the competitive antagonist 4OH-GTS-21, obtained by DOCK6.1 calculation.

formed in one subtype whereas the −NH group on the indole ring of Trp may donate a hydrogen bond in the alternate subtype. In the model of 4OH-GTS-21 docked in the LBD of wild-type α4β2, Trp55 is localized in such a position that its bulkiness seems to be a primary cause for forcing an unreasonable twist of the benzylidene group's double bond (Fig. 8). If compounds like 4OH-GTS-21 bind with the benzylidene group in a position similar to that modeled, the mutation of Trp55/Trp57 may significantly alter ligand-receptor interactions on the complementary face in a receptor subtype-dependent fashion. The observation that α4β2 receptors gain function with 4OH-GTS-21 when Trp57 is mutated to smaller residues is consistent with the idea that the wild-type receptor has unfavorable steric clashes with this compound. In the case of the α7 receptor, the interactions of 4OH-GTS-21 with Trp55 may be optimum, such that in general, making this position smaller in size results in less favorable binding and/or function. The increase in 4OH-GTS-21 efficacy observed in W55V mutants may result from the β branching of Val, which confers sufficient size that receptor function is maintained or, in this case, potentiated relative to ACh responses.

The possibility that 4OH-GTS-21 is capable of interacting with nicotinic receptors in unique ways to induce receptor activation cannot be ruled out, suggesting a given ligand may have multiple alternative binding conformations. In one receptor subtype, the conformations that can catalyze gating may be favored over alternative conformations that do not. Mutations such as the β2W57Y may alter the preferred binding of 4OH-GTS-21, increasing probability that gating will occur. In the current study, 4OH-GTS-21 is the only agonist we tested that efficaciously activated certain α4β2 mutants while losing α7 efficacy. Likewise, in the previous study with Y188F mutants, anabaseine derivatives were the only α7 agonists tested that activated the mutant α4β2 receptors, with 4OH-GTS-21 being the most efficacious by far (Horenstein et al., 2007). These observations raise questions regarding how 4OH-GTS-21 activates the nAChR. Although it is possible that 4OH-GTS-21 may fit into the binding site of wild-type α7 and α4β2 in different conformations, it is also likely that ligands such as ACh and 4OH-GTS-21 form different types of intermolecular interactions with residues in the protein, thereby promoting receptor activation in different ways. Investigations of AChBP bound with agonists and antagonists have led to the idea that channel opening and, possibly, ligand selectivity may occur through a conformation induced by the ligand, which is due to the inherent flexibility of the binding site, allowing it to conform to the structural characteristics of the ligand (Hansen et al., 2005). A potentially important observation is that acetylcholine, choline, and AR-R17779 all contain sp^3 hybridized ammonium nitrogen atoms; hence, the onium substituent groups occupy space in three dimensions. The onium nitrogen atom thought to be important in 4OH-GTS-21 binding is sp^2 hybridized and flat, resulting in a lower steric demand. This difference in three-dimensional structure among choline, AR-R17779, and 4OH-GTS-21 may underlie some of the unique observations made in this study regarding 4OH-GTS-21. Work is in progress to further explore this hypothesis via homology modeling and comparative docking studies of these alternate agonists.

In contrast to the variable effects of Trp55 mutations, Trp149 seems to serve more like a structural "pillar" in the LBD (Fig. 9), universally important for receptor function, regardless of agonist or receptor subtype. However, if Trp149 were solely responsible for stabilizing the ligand, one would expect to see total loss of receptor activity when this residue became incapable of forming cation-π interactions. This clearly was not the case because the nonaromatic α7 Trp149 mutant receptors still responded to agonists, and mutation to other aromatic residues actually produced receptors that were nonresponsive to ACh. Other aromatic residues and nonaromatic residues found within the LBD probably help to stabilize and compensate for lost interactions resulting from mutation or perhaps form an alternate set of interactions with ACh that are still capable of activating the receptor when the Trp149 is mutated. As shown in Fig. 8, the LBD places three electron-rich Tyr residues around the cationic ammonium center. These groups may compensate for the mutation of Trp149 in regard to cation recognition in the Trp149 mutants that were functional. One general observation that may be made from the homology modeling is that the conserved Trp149 is placed in an ideal position to affect receptor structure and function because it effectively lines the LBD pocket under the C-loop, providing a large hydrophobic face to this pocket. Mutations here may have a general deleterious effect because they disrupt this core part of the LBD. If the fulcrum-and-pillar hypothesis is correct, residues localized in the vicinity of the LBD may establish interactions with the ligand that place it in a position in

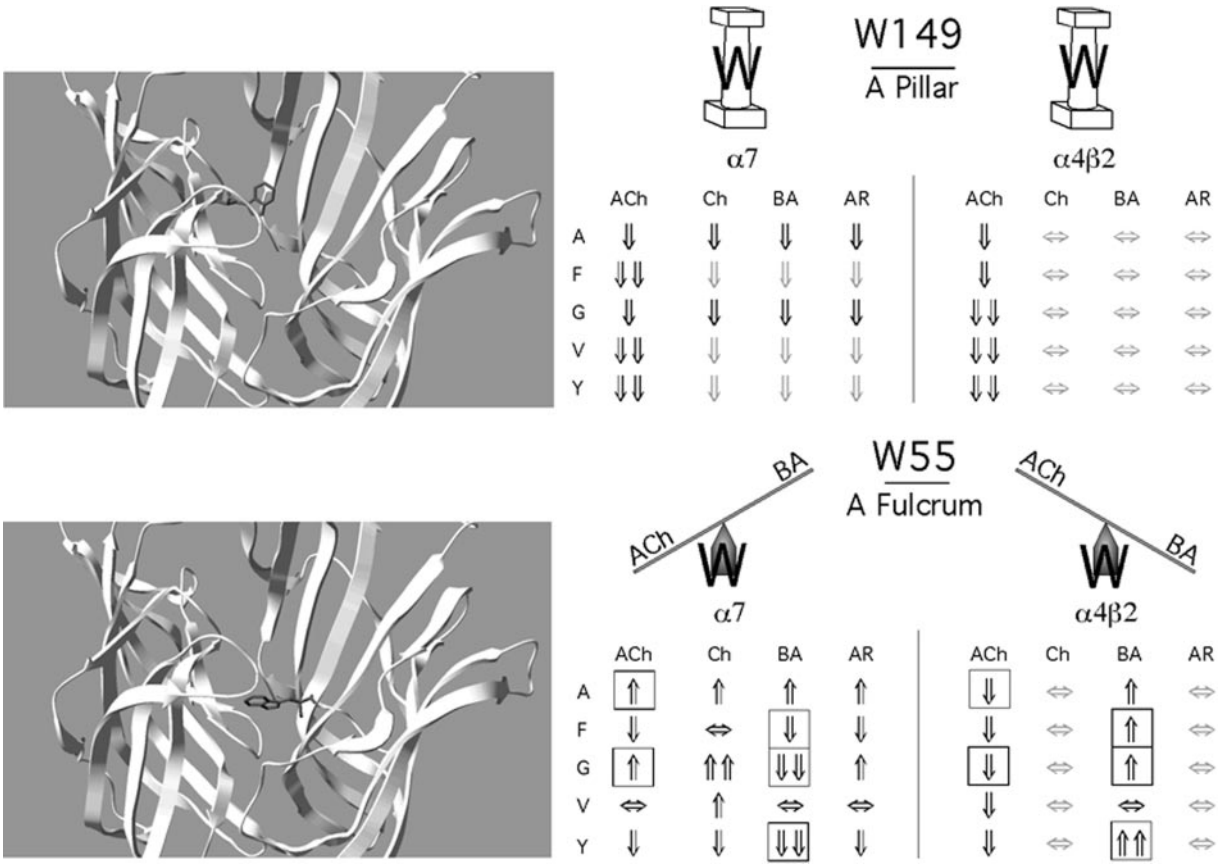

Fig. 9. Conserved residues in the nAChR LBD function as pillars or fulcrums. The Trp149 of α7 and the homologous residue in α4 are of critical importance for activation of both subtypes by ACh, and in α7, for activation by the subtype-selective agonists tested: choline (Ch), 4OH-GTS-21 (BA), and AR-R17779 (AR). The down arrows represent the reduced activation observed with all of the Trp149 mutants tested. Grayed arrows represent responses to subtype-selective agonists that were reduced below the level of detection. Horizontal arrows represent responses that were unchanged by mutations, and grayed horizontal arrows represent subthreshold responses below the limit of detection in both wild-type and mutant α4β2 receptors. In contrast, Trp55 of α7 and the homologous residue (Trp57) in β2 are critical determinants of the unique pharmacology of the α7 and α4β2 receptor subtypes. In α7, Trp55 seems to be important for activation by the subtype-selective agonists in balance with ACh. Mutations of Trp57 in β2 can make the receptors available for activation by 4OH-GTS-21 while at the same time reducing responses to ACh compared with wild type. Boxes, mutations that have opposite effects in α7 and α4β2.

which its ability to interact with the receptor and initiate changes in channel gating is regulated by conserved amino acids such as Trp55 or Tyr188 (α7 numbering). Identification of other residues that may contribute to the ability of conserved residues to regulate receptor activation by subtype-selective agonists is an important topic of future research.

Adding insight to the results presented here is the report that serotonin activates the highly homologous mouse 5HT3 and *Caenorhabditis elegans* MOD-1 receptors through formation of cation-π interactions at different Trp residues, at the position homologous to Trp149 in 5HT3, and at the position homologous to Tyr195 in MOD-1. In MOD-1, the residues at the positions homologous to 149 and 195 in α7 are Tyr and Trp, respectively (Mu et al., 2003). Mutation of these residues suggested that both receptors make specific contacts with serotonin that regulate channel gating, but those specific contacts depend on the nature of the binding site. Evolutionary pressures may have allowed some flexibility in the ability of conserved aromatic residues to act differentially in different receptors, or serotonin may be accommodating to the distinct binding domains, finding alternate ways to establish interactions that lead to receptor activation. In conclusion, our data augment the existing evidence that structurally distinct agonists are capable of activating receptors in unique ways and provide new details regarding possible mechanisms of α7-selective nAChR activation and agonist selectivity.

Acknowledgments

We thank Lisa Jacobs, Lynda Cortes, Sara Braley, and Shehd Al Rubaiy for technical assistance.

References

Arnold K, Bordoli L, Kopp J, and Schwede T (2006) The SWISS-MODEL workspace: a web-based environment for protein structure homology modelling. *Bioinformatics* **22:**195–201.

Aylwin ML and White MM (1994) Ligand-receptor interactions in the nicotinic acetylcholine receptor probed using multiple substitutions at conserved tyrosines on the alpha subunit. *FEBS Lett* **349:**99–103.

Brejc K, van Dijk WJ, Klaassen RV, Schuurmans M, van Der Oost J, Smit AB, and Sixma TK (2001) Crystal structure of an ACh-binding protein reveals the ligand-binding domain of nicotinic receptors. *Nature* **411:**269–276.

Celie PH, van Rossum-Fikkert SE, van Dijk WJ, Brejc K, Smit AB, and Sixma TK (2004) Nicotine and carbamylcholine binding to nicotinic acetylcholine receptors as studied in AChBP crystal structures. *Neuron* **41:**907–914.

Chiara DC and Cohen JB (1997) Identification of amino acids contributing to high and low affinity D-tubocurarine sites in the Torpedo nicotinic acetylcholine receptor. *J Biol Chem* **272:**32940–32950.

Chiara DC, Middleton RE, and Cohen JB (1998) Identification of tryptophan 55 as the primary site of [3H]nicotine photoincorporation in the gamma-subunit of the Torpedo nicotinic acetylcholine receptor. *FEBS Lett* **423:**223–226.

Cohen JB, Sharp SD, and Liu WS (1991) Structure of the agonist-binding site of the nicotinic acetylcholine receptor: [^{3}H]acetylcholine mustard identifies residues in the cation-binding subsite. *J Biol Chem* **266:**23354–23364.

Dani JA and Bertrand D (2007) Nicotinic acetylcholine receptors and nicotinic cholinergic mechanisms of the central nervous system. *Annu Rev Pharmacol Toxicol* **47:**699–729.

Devillers-Thiéry A, Galzi JL, Eiselé JL, Bertrand S, Bertrand D, and Changeux JP (1993) Functional architecture of the nicotinic acetylcholine receptor: a prototype of ligand-gated ion channels. *J Membr Biol* **136:**97–112.
Francis MM, Cheng EY, Weiland GA, and Oswald RE (2001) Specific activation of the alpha 7 nicotinic acetylcholine receptor by a quaternary analog of cocaine. *Mol Pharmacol* **60:**71–79.
Galzi JL, Bertrand D, Devillers-Thiéry A, Revah F, Bertrand S, and Changeux JP (1991) Functional significance of aromatic amino acids from three peptide loops of the alpha 7 neuronal nicotinic receptor site investigated by site-directed mutagenesis. *FEBS Lett* **294:**198–202.
Galzi JL and Changeux JP (1995) Neuronal nicotinic receptors: molecular organization and regulations. *Neuropharmacology* **34:**563–582.
Gay EA, Giniatullin R, Skorinkin A, and Yakel JL (2008) Aromatic residues at position 55 of rat alpha7 nicotinic acetylcholine receptors are critical for maintaining rapid desensitization. *J Physiol* **586:**1105–1115.
Gotti C, Zoli M, and Clementi F (2006) Brain nicotinic acetylcholine receptors: native subtypes and their relevance. *Trends Pharmacol Sci* **27:**482–491.
Halevi S, Yassin L, Eshel M, Sala F, Sala S, Criado M, and Treinin M (2003) Conservation within the RIC-3 gene family: effectors of mammalian nicotinic acetylcholine receptor expression. *J Biol Chem* **278:**34411–34417.
Hansen SB, Sulzenbacher G, Huxford T, Marchot P, Taylor P, and Bourne Y (2005) Structures of Aplysia AChBP complexes with nicotinic agonists and antagonists reveal distinctive binding interfaces and conformations. *EMBO J* **24:**3635–3646.
Hansen SB and Taylor P (2007) Galanthamine and non-competitive inhibitor binding to ACh-binding protein: evidence for a binding site on non-alpha-subunit interfaces of heteromeric neuronal nicotinic receptors. *J Mol Biol* **369:**895–901.
Higgins DG, Thompson JD, and Gibson TJ (1996) Using CLUSTAL for multiple sequence alignments. *Methods Enzymol* **266:**383–402.
Horenstein NA, McCormack TJ, Stokes C, Ren K, and Papke RL (2007) Reversal of agonist selectivity by mutations of conserved amino acids in the binding site of nicotinic acetylcholine receptors. *J Biol Chem* **282:**5899–5909.
Kalamida D, Poulas K, Avramopoulou V, Fostieri E, Lagoumintzis G, Lazaridis K, Sideri A, Zouridakis M, and Tzartos SJ (2007) Muscle and neuronal nicotinic acetylcholine receptors: structure, function and pathogenicity. *FEBS J* **274:**3799–3845.
Kopp J and Schwede T (2004) The SWISS-MODEL Repository of annotated three-dimensional protein structure homology models. *Nucleic Acids Res* **32:**D230–D234.
Kuryatov A, Onksen J, and Lindstrom J (2008) Roles of accessory subunits in alpha4beta2(*) nicotinic receptors. *Mol Pharmacol* **74:**132–143.
Moustakas DT, Lang PT, Pegg S, Pettersen E, Kuntz ID, Brooijmans N, and Rizzo RC (2006) Development and validation of a modular, extensible docking program: DOCK 5. *J Comput Aided Mol Des* **20:**601–619.
Mu TW, Lester HA, and Dougherty DA (2003) Different binding orientations for the same agonist at homologous receptors: a lock and key or a simple wedge? *J Am Chem Soc* **125:**6850–6851.
O'Leary ME and White MM (1992) Mutational analysis of ligand-induced activation of the Torpedo acetylcholine receptor. *J Biol Chem* **267:**8360–8365.
Ortells MO and Lunt GG (1995) Evolutionary history of the ligand-gated ion-channel superfamily of receptors. *Trends Neurosci* **18:**121–127.
Papke RL (2006) Estimation of both the potency and efficacy of alpha7 nAChR agonists from single-concentration responses. *Life Sci* **78:**2812–2819.
Papke RL and Porter Papke JK (2002) Comparative pharmacology of rat and human alpha7 nAChR conducted with net charge analysis. *Br J Pharmacol* **137:**49–61.
Papke RL, Kem WR, Soti F, Lopez-Hernandez GY, and Horenstein NA (2009) Activation and densensitization of nicotinic α7-type acetylcholine receptors by benzylidene anabaseines and nicotine. *J Pharmacol Exp Ther* **329:**791–807.
Papke RL and Thinschmidt JS (1998) The correction of alpha7 nicotinic acetylcholine receptor concentration-response relationships in *Xenopus* oocytes. *Neurosci Lett* **256:**163–166.
Pettersen EF, Goddard TD, Huang CC, Couch GS, Greenblatt DM, Meng EC, and Ferrin TE (2004) UCSF Chimera: a visualization system for exploratory research and analysis. *J Comput Chem* **25:**1605–1612.
Schwede T, Kopp J, Guex N, and Peitsch MC (2003) SWISS-MODEL: an automated protein homology-modeling server. *Nucleic Acids Res* **31:**3381–3385.
Sine SM, Quiram P, Papanikolaou F, Kreienkamp HJ, and Taylor P (1994) Conserved tyrosines in the alpha subunit of the nicotinic acetylcholine receptor stabilize quaternary ammonium groups of agonists and curariform antagonists. *J Biol Chem* **269:**8808–8816.
Tasneem A, Iyer LM, Jakobsson E, and Aravind L (2005) Identification of the prokaryotic ligand-gated ion channels and their implications for the mechanisms and origins of animal Cys-loop ion channels. *Genome Biol* **6:**R4.
Tomaselli GF, McLaughlin JT, Jurman ME, Hawrot E, and Yellen G (1991) Mutations affecting the agonist sensitivity of the nicotinic acetylcholine receptor. *Biophys J* **60:**721–727.
Xie Y and Cohen JB (2001) Contributions of Torpedo nicotinic acetylcholine receptor gamma Trp-55 and delta Trp-57 to agonist and competitive antagonist function. *J Biol Chem* **276:**2417–2426.
Xiu X, Puskar NL, Shanata JA, Lester HA, and Dougherty DA (2009) Nicotine binding to brain receptors requires a strong cation-pi interaction. *Nature* **4587:**534–537.
Zhong W, Gallivan JP, Zhang Y, Li L, Lester HA, and Dougherty DA (1998) From ab initio quantum mechanics to molecular neurobiology: a cation-pi binding site in the nicotinic receptor. *Proc Natl Acad Sci U S A* **95:**12088–12093.

Address correspondence to: Roger L. Papke, Department of Pharmacology and Therapeutics, University of Florida, P.O. Box 100267, Gainesville, FL 32610-0267. E-mail: rlpapke@ufl.edu